Available online at www.sciencedirect.com
SCIENCE DIRECT®
Journal of Sound and Vibration 285 (2005) 425–442
JOURNAL OF SOUND AND VIBRATION
www.elsevier.com/locate/jsvi

Transverse shear modulus identification by an inverse method using measured flexural resonance frequencies from beams

Yinming Shi[a,b,*], Hugo Sol[b], Hongxing Hua[a]

[a]*The State Key Lab for Vibration, Shock and Noise, Shanghai Jiao Tong University, Shanghai, China*
[b]*Department of Mechanics of Material and Construction, Vrije Universiteit Brussel, Pleinlaan 2, B-1050 Brussels, Belgium*

Received 10 November 2003; received in revised form 23 March 2004; accepted 29 March 2004

Abstract

Many papers have already been presented about identification of 2D in plane elastic engineering constants E1, E2, v12 and G12 by inverse methods. Most of the described methods are based on measured resonance frequencies on plate specimens. Less attention has been paid to the identification of transverse shear moduli. Especially, validation of the obtained results and error bound estimations are often lacking. This paper presents an inverse method for the identification of the transverse moduli of test beams by measured flexural resonance frequencies. The procedure is first illustrated with numerically generated test data and next applied on experimentally measured results. The sensitivity of the flexural resonance frequencies for variations of the shear modulus is discussed as well as an estimation of the uncertainty intervals on the obtained moduli. The results are validated by using the obtained shear moduli for the prediction of torsional resonance frequencies.

1. Introduction

Elastic engineering constants are usually determined by static test methods like tensile, bending, torsion and shear testing. Many standard tests are described in literature and have proven their

*Corresponding author. Fax: +32-2-629-2928.
E-mail address: yinming.shi@vub.ac.be (Y. Shi).

0022-460X/$ - see front matter © 2004 Elsevier Ltd. All rights reserved.
doi:10.1016/j.jsv.2004.03.074

validity through engineering history. Standard static test methods, however, show some drawbacks, among which the following:

- Uniform stress/strain fields are assumed for the computation of the elastic moduli. Due to boundary conditions (like clamps and supports), misalignments, geometrical imperfections and anisotropic coupling effects, the real stress/strain fields are far from perfectly uniform.
- Many methods are based on locally measured strains and thus are vulnerable to material heterogeneities. Test results on fiber-reinforced composite materials for example often exhibit large scatter for this reason.

Methods based on measured resonance frequencies of free–free specimens do not suffer from the above-mentioned disadvantages. Resonance frequencies are global properties of the specimens and wavelengths of the considered modes are usually much larger than the scale of material heterogeneities in the specimen. Resonance frequency methods hence provide results averaged over the whole volume of the specimen. By measuring several frequencies associated with different mode shapes, homogenization is enhanced and redundancy is created.

The principle of inverse methods for material identification is to update iteratively the engineering constants in a finite element model of the test specimens in such a way that the computed frequencies match the measured frequencies (see Fig. 1).

The engineering constants that minimize an output residual are considered as the solution of the procedure. The minimization of the output residual is realized by optimization methods that minimize a scalar value called ''the objective function''. A typical objective function is the sum of the squared residual components.

The underlying idea of inverse methods that are based on measurement of resonance frequencies originates from the observation that all constructions made with elastic materials have a characteristic set of resonance frequencies. The value of these frequencies is determined by the geometry, boundary conditions, the elastic moduli and the density of the used materials. Thus,

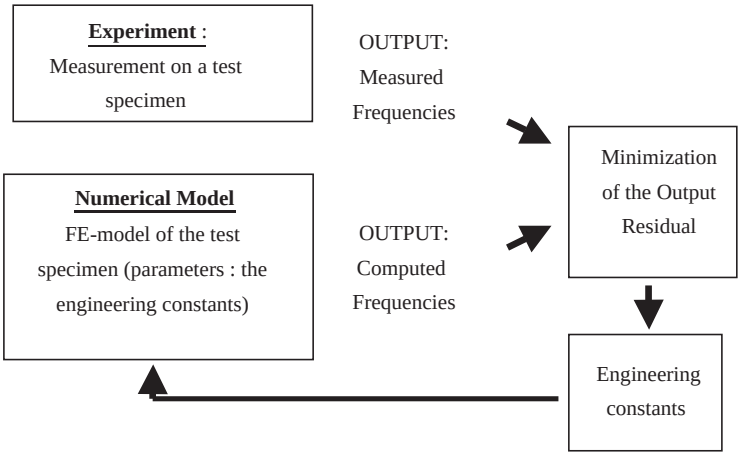

Fig. 1. Principle of an inverse method using measured frequencies.

inversely, these resonance frequencies can be used as tools to determine the elastic moduli if the geometry, boundary conditions and the density are assumed to be known.

The first attempt of identification of material properties by an inverse method using vibration data was proposed by Wolf and Carne in 1979 [1]. They used an empirical plate model of an isotropic plate specimen with free edges. In 1982, De Wilde and Sol [2–4] used finite element models and measured resonance frequencies to identify plate rigidities of anisotropic thin plates. In 1985, Deobald [5,6] used a modal analysis/Rayleigh–Ritz technique of an orthotropic rectangular plate to obtain estimated values of plates rigidities from measured resonance frequencies. Frederiksen also applied the same method on identification of material parameters [7] from thin plates. In 1991, Carne and Martinez identified the elastic material constants of shell structures [8]. In 1993, Moussu and Nivoit [9] used a modal analysis/method of superposition to determine the elastic engineering constants of orthotropic thin plates from measured frequencies. They claimed that the proposed superposition method provided fast and accurate eigenvalues of orthotropic plates. In 1999, T. C. Lai and Ip [10] used Bayesian sensitivity analysis/Rayleigh–Ritz method to identify the material properties of orthotropic rectangular thin plate with completely free boundary conditions.

All the above methods are based on the classical Kirchhoff thin plate theory. The influence of the transverse shear moduli (G_{13}, G_{23}) was ignored. In order to identify the shear moduli, Hua [11] studied several models of thick plates and statistical updating methods. In 1995, Frederiksen [12] extended his work from thin plates to thick plates. He used a high-order shear deformation theory [13]. In 1996, Marchand, and Authesserre [14] used a statistical analysis method to identify Young's moduli and Poisson's ratio of metals based on a Mindlin theory applied on a circular plate. They also investigated the influence of temperature on the value of Young's modulus. In 1996, Grédiac and Paris [15] proposed a virtual displacement method to determine material constants from measured frequencies and modal shapes of a plate. The proposed method needed no initial values and no iterations. In 2000, Wang and Kam [16] used a first-order shear deformation theory and an optimization program to identify transverse shear moduli. In 2000, Hwang and Chang [17] used Kirchhoff thin plate elements and Mindlin moderate thick plate elements to build a numerical plate model and used a derivation-based optimization procedure to identify the transverse shear modulus. In 2001, Rikards et al. [18] combined a finite element method with model reduction to obtain a mathematical model of a moderate thick plate. The response surface method was used to optimize the identification function. In 2002, Liu et al. [19] used a progressive neutral network (NN) to derive material constants from measured displacements. The method seemed very interesting, but it appeared to be very difficult to train an NN model for the complex relationship between material properties and dynamic responses in a wide range of parameters.

A major problem for the identification of transverse shear modulus is the fact that the frequencies are not sensitive to variations of the transverse shear modulus in plates. Even for a relatively thick plate, it appeared to be very difficult to identify accurately the shear modulus from a set of measured frequencies. Therefore, some people tended to use beam specimens for the identification of the transverse shear modulus. The ASME standard [20] proposes a procedure to determine material parameters from test beams, but unfortunately, it is only suitable for isotropic material with an assumed relation between Young's modulus, Poisson's ratio and the shear modulus.

In 1990, Larsson [21] proposed a procedure to determine the transverse shear modulus of beams by a kind of diagram method. However, this method appeared to be not convenient for shear modulus identification. Wanner and Kromp [22] used five flexural frequencies to identify Young's modulus and the shear modulus based on approximate Timoshenko beam formulas. The obtained Young's modulus was accurate, but the accuracy of the shear modulus was not so good. In 1999, Lins [23] built a new equipment to identify G at up to a temperature of 2000°C. This method was based on solving the Timoshenko beam characteristic equation with a free–free boundary equation. Since this characteristic equation is a transcendental equation, it is not so easy and convenient to find the correct roots. Using numerical methods to solve the transcendental equation, the accuracy of the obtained shear modulus is in the same order of magnitude as the results found by Wanner [22].

The goal of this paper is to find a convenient, accurate and simple way to identify the shear modulus. Therefore an inverse method is selected as the identification tool. The shear modulus identified from formulas based on Timoshenko beam theory is used as initial value. The used finite element model is based on Timoshenko beam theory and the Nelder–Mead Simplex (NMSPX) optimization method [24] is selected as optimization algorithm. Some numerical examples and experiments are given to illustrate and validate the method. At the end of the paper an error discussion is given. The first paragraph starts with an overview of the influence of the shear modulus on flexural beam resonance frequencies.

2. Transverse shear modulus identification by an inverse method

In order to find the transverse shear modulus using an inverse method, several items must be selected: an accurate numerical model, good initial values, a suitable objective function and a performing optimization program. The next paragraphs will describe these items one by one in some detail.

2.1. The finite element model

The correct identification of the material properties with an inverse method requires an accurate mathematical model. In this section, a finite element model based on the Timoshenko beam theory is developed. The Timoshenko beam theory takes deformations due to transverse shear into account in a linearized way. Fig. 2 presents the selected 3 node element.

The column of nodal displacements becomes:

$$\delta^e = [w_1 \;\; \theta_1 \;\; w_2 \;\; \theta_2 \;\; w_3 \;\; \theta_3]^{\mathrm{T}}. \tag{1}$$

The shape functions associated to these 3 nodes are expressed in reduced coordinates:

$$\begin{aligned} N_1 &= -\tfrac{1}{2}\xi(1-\xi), \\ N_2 &= (1-\xi)\xi(1+\xi), \\ N_3 &= -\tfrac{1}{2}\xi(1+\xi). \end{aligned} \tag{2}$$

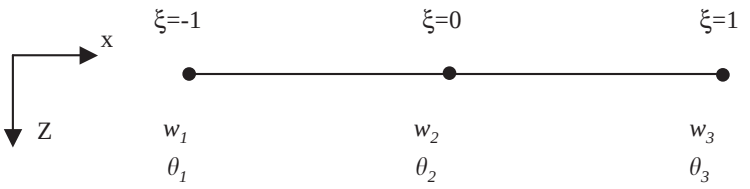

Fig. 2. Parabolic (3 node) Timoshenko beam element.

The displacement and the rotation at any point within the element can be evaluated with

$$w = \sum_{i=1}^{3} N_i w_i, \tag{3}$$

$$\theta = \sum_{i=1}^{3} N_i \theta_i. \tag{4}$$

The x coordinates can be found by isoparametrical mapping of the reduced coordinates:

$$x = \sum_{i=1}^{3} N_i x_i. \tag{5}$$

The potential energy equation is

$$E_p = \frac{1}{2} \int_{L/2}^{L/2} \left[\int_A Ez^2 \left(\frac{\partial \theta}{\partial x} \right)^2 \mathrm{d}A + \int_A \sigma_{xz} \left(-\theta + \frac{\partial w}{\partial x} \right) \mathrm{d}A \right] \mathrm{d}x. \tag{6}$$

In order to account for the fact that shear stress is a parabolic distribution on a cross-section, it is common to introduce a cross-section reduction factor K' in such a way that

$$\int_A \sigma_{xz} dA = K' A G \gamma_{xz},$$

where A is the cross-section area and G is the shear moduli of the material. Eq. (6) becomes

$$E_p = \frac{1}{2} \int_{L/2}^{L/2} \left[EI \left(\frac{\partial \theta}{\partial x} \right)^2 + K' A G \left(-\theta + \frac{\partial w}{\partial x} \right)^2 \right] \mathrm{d}x. \tag{7}$$

where E is Young's modulus. I is the moment of area. K' is $\frac{5}{6}$ for beams with rectangle cross-section. The kinetic energy is

$$\begin{aligned} E_k &= \frac{1}{2} \int_{L/2}^{L/2} \left[\int_A \rho (\dot{u}^2 + \dot{w}^2) \, \mathrm{d}A \right] \mathrm{d}x \\ &= \frac{1}{2} \int_{L/2}^{L/2} \left[\rho I \dot{\theta}^2 + \rho A \dot{w}^2 \right] \mathrm{d}x. \end{aligned}$$

The stiffness matrix K and mass matrix M can be derived from the above formulas with standard finite element procedures. The above-described finite element model was programmed on the cryptic platform MATLAB.

2.2. Initial values

For beams with rectangular cross-sections, formulas [22] proposed by Wanner and Kromp can be used to calculate good initial values of Young's modulus E and transverse shear modulus G:

$$E_{TIM} = A_n + B_n \frac{E_{TIM}}{G} \tag{8}$$

with

$$A_n = E_{BE}\left(1 + a_n \frac{t^2}{L^2}\right),$$

$$B_n = E_{BE}\left(b_n \frac{t^2}{L^2} - c_n \frac{t^4}{L^4}\right),$$

$$E_{BE} = \frac{48\rho\pi^2 L^4}{t^2 m_n^4} f_n^2.$$

Table 1 lists the constants in the above formulas for the first six flexural mode shape numbers.

Eq. (8) is used to obtain Young's modulus E_{TIM} and transverse shear modulus G. Eq. (8) must be evaluated for at least two different sets of values. Different sets can be generated by varying the length-to-thickness ratio for the same mode number or by selecting other mode shape numbers.

2.3. Optimization process

Optimization methods can minimize the output residual in an inverse method by the selection of an adequate scalar objective function that contains the residual as a variable. The objective function selected in this paper can be written as

$$\text{Objective Function} = \sum_{i=1}^{N} \left(1 - \frac{f_{iA}}{f_{iE}}\right)^2. \tag{9}$$

Table 1
Constants of free–free Timoshenko beam formulas

Mode No. n	M_n	A_n	B_n	C_n
1	4.7300	4.12	1.23	4.20
2	7.8532	9.08	4.60	32.0
3	10.996	15.6	9.89	122
4	14.137	23.7	17.2	333
5	17.279	33.5	26.4	746
6	20.420	45.0	37.6	1449

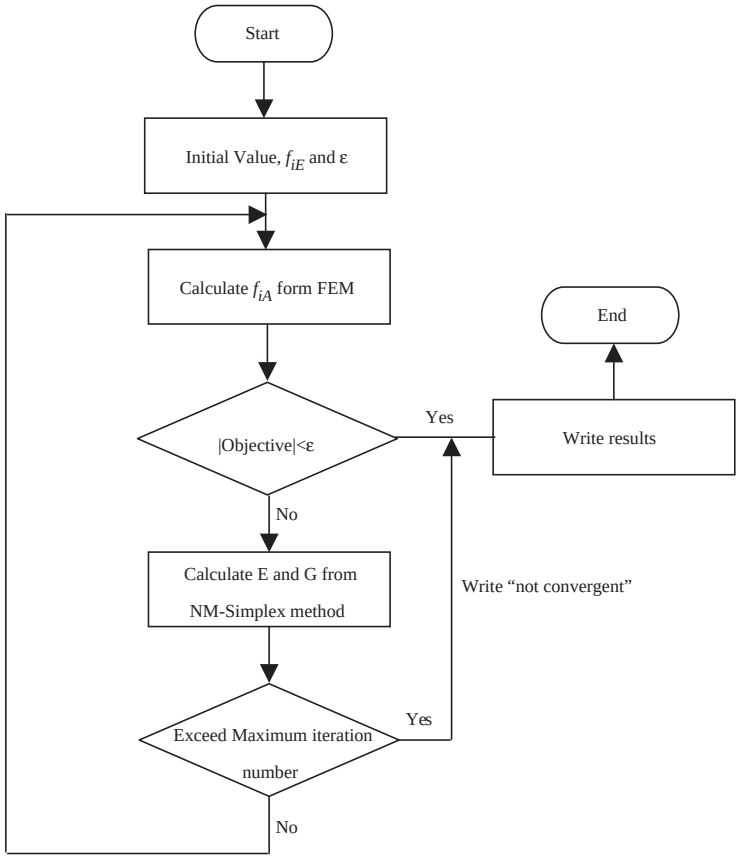

Fig. 3. Flowchart of the whole identification process.

f_{iA} are the ith calculated frequencies with the finite element program and f_{iE} are the experimentally measured ith frequencies. N is the total number of considered frequencies.

A direct search method called the NM SPX optimization method [24] is selected in this paper. Fig. 3 shows the flowchart for the complete identification process.

3. Error estimation

3.1. Theoretical derivation of the uncertainty bounds

Consider a numerical model of a test specimen with a relationship between n frequencies, r target parameters (such as Young's moduli, shear moduli) and s test specimen parameters (such as lengths, thicknesses, widths and masses). At given target and test specimen parameter values, finite uncertainty intervals of frequency valves due to finite target and test specimen uncertainty

intervals can be approximated as

$$\begin{Bmatrix} \Delta f_1 \\ \Delta f_2 \\ \vdots \\ \Delta f_n \end{Bmatrix} = \begin{bmatrix} \frac{\partial f_1}{\partial p_1} & \frac{\partial f_1}{\partial p_2} & \cdots & \frac{\partial f_1}{\partial p_r} & \frac{\partial f_1}{\partial g_1} & \frac{\partial f_1}{\partial g_2} & \cdots & \frac{\partial f_1}{\partial g_s} \\ \frac{\partial f_2}{\partial p_1} & \frac{\partial f_2}{\partial p_2} & \cdots & \frac{\partial f_2}{\partial p_r} & \frac{\partial f_2}{\partial g_1} & \frac{\partial f_2}{\partial g_2} & \cdots & \frac{\partial f_2}{\partial g_s} \\ \vdots & \vdots & \cdots & \vdots & \vdots & \vdots & \cdots & \vdots \\ \frac{\partial f_n}{\partial p_1} & \frac{\partial f_n}{\partial p_2} & \cdots & \frac{\partial f_n}{\partial p_r} & \frac{\partial f_n}{\partial g_1} & \frac{\partial f_n}{\partial g_2} & \cdots & \frac{\partial f_n}{\partial g_s} \end{bmatrix} \begin{Bmatrix} \Delta p_1 \\ \Delta p_2 \\ \vdots \\ \Delta p_r \\ \Delta g_1 \\ \Delta g_2 \\ \vdots \\ \Delta g_s \end{Bmatrix}. \tag{10}$$

The input parameters for the inverse method are the n frequencies and s test specimen parameters. The relative uncertainties Δp on the r target parameters due to the uncertainties on the $n+s$ input parameters can be computed as [25–28]

$$\Delta p = \begin{bmatrix} s_p^+ & -s_p^+ \cdot s_g \end{bmatrix} \begin{Bmatrix} \Delta f \\ \Delta g \end{Bmatrix}, \tag{11}$$

where

$$s_p^+ \text{ is the pseudo inverse of } s_p$$

and

$$s_p = \begin{bmatrix} \frac{\partial f_1}{\partial p_1} & \frac{\partial f_1}{\partial p_2} & \cdots & \frac{\partial f_1}{\partial p_r} \\ \frac{\partial f_2}{\partial p_1} & \frac{\partial f_2}{\partial p_2} & \cdots & \frac{\partial f_2}{\partial p_r} \\ \vdots & \vdots & \vdots & \vdots \\ \frac{\partial f_n}{\partial p_1} & \frac{\partial f_n}{\partial p_2} & \cdots & \frac{\partial f_n}{\partial p_r} \end{bmatrix}, s_g = \begin{bmatrix} \frac{\partial f_1}{\partial g_1} & \frac{\partial f_1}{\partial g_2} & \cdots & \frac{\partial f_1}{\partial g_s} \\ \frac{\partial f_2}{\partial g_1} & \frac{\partial f_2}{\partial g_2} & \cdots & \frac{\partial f_2}{\partial g_s} \\ \vdots & \vdots & \vdots & \vdots \\ \frac{\partial f_n}{\partial g_1} & \frac{\partial f_n}{\partial g_2} & \cdots & \frac{\partial f_n}{\partial g_s} \end{bmatrix}. \tag{12}$$

The uncertainty intervals of the input parameters can be stored in a global column $\{\Delta m\} = \begin{Bmatrix} \Delta f \\ \Delta g \end{Bmatrix}$. The relative contribution of the uncertainty of the jth input parameter on the uncertainty of the ith identified material parameter can be computed [25–28]:

$$\rho_{ij} = \frac{|s_{ij}| \cdot \Delta m_j}{\sum_{j=1}^{n+s} |s_{ij}| \cdot \Delta m_j}, \quad i = 1, 2, \ldots, r, \tag{13}$$

with

$$[s] = \begin{bmatrix} s_p^+ & -s_p^+ \cdot s_g \end{bmatrix}. \tag{14}$$

The relation (13) satisfies the consistency condition:

$$\sum_{j=1}^{n+s} \rho_{ij} = 1, \quad i = 1, 2, \ldots, r. \tag{15}$$

3.2. Numerical simulations of the uncertainty bounds

In this section, a group of beams is used to map graphically the uncertainty of the identified material parameters E and G due to uncertainties of measured frequencies, length, width, thickness and mass. The uncertainty of the identified parameters is numerically studied in the function of dimensionless parameters E/G (Young's modulus divided by the shear modulus) and L/t (Length-to-thickness ratio). The reference properties of the studied beams are arbitrary selected: a thickness of 0.005 m, a width of 0.01 m, a Young's modulus of 2.7E + 10 Pa and a density of 1500 kg/m^3. The studied beams have all the same reference thickness, width, Young's modulus and density, but they have varying lengths and transverse shear moduli. The ratio between the length and thickness has been varied from 10 to 150. The ratio between Young's modulus and the transverse shear modulus varied from 2 to 50. The assumed uncertainties of the input parameters are listed in Table 2. According to formulas (11) and (13) in Section 3.1, the relative errors between the uncertainties of material properties and their corresponding identified values are calculated. Figs. 4 and 5 show the obtained results.

It can be seen from Fig. 4 that, even for a relatively small uncertainty of the input parameters, the uncertainty of G for beams with a big L/T ratio and a low E/G ratio can be considerable. For those slender beams, the influence of G on the frequencies is little and consequently the uncertainty on the obtained G-value becomes high. On the contrary, the obtained uncertainty of G for the beams with a small L/T ratio and a high E/G ratio is quite small. For those short beams, the influence of G on the resonance frequencies is obvious. It can be concluded that a sufficient influence of G on the frequencies is necessary to obtain acceptable small uncertainties on the identified G-values.

It can be seen from Fig. 5 that the uncertainties on the identified Young's modulus are much more constant and low. The relative errors are smaller than 1.5%. The smallest relative errors are obtained from beams, whose L/T is about 50. For slender beams (L/T is bigger than 50), the frequencies are low and the uncertainties on the measured frequencies become dominant. On the contrary, for short beams (L/T is much smaller than 50), the frequencies are higher and this time the uncertainties of measured geometric parameters such as thickness, length, width and weight become dominant.

Table 2
The assumed uncertainties on the "measured" input parameters

Parameters	Freq-1 (Hz)	Freq-2 (Hz)	Freq-3 (Hz)	Freq-4 (Hz)	Freq-5 (Hz)	Freq-6 (Hz)	Freq-7 (Hz)	Length (mm)	Width (mm)	Thickness (mm)	Mass (g)
Uncertainties	±0.1	±0.1	±0.1	±0.5	±0.5	±1	±1	±0.01	±0.01	±0.01	±0.01

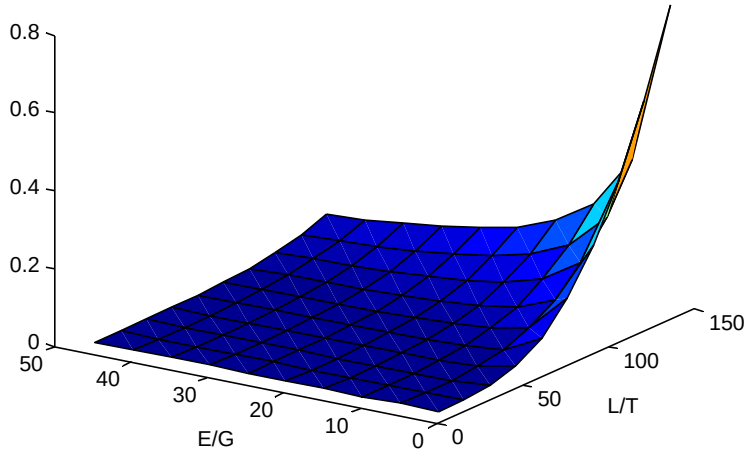

Fig. 4. Relative error (uncertainty) of the identified G-value.

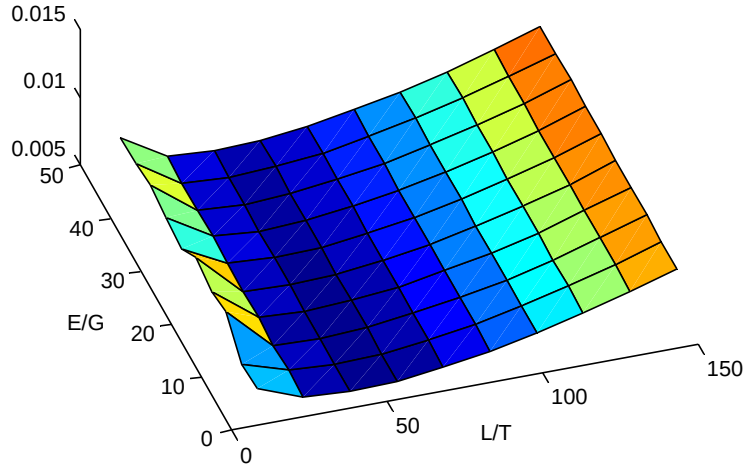

Fig. 5. Relative error (uncertainty) of the identified E-value.

4. Numerical examples

4.1. Numerical example 1

A first step in checking the performance of the inverse method is using "virtual experimental frequencies" generated with its own numerical model. Hence all experimental errors and model errors are eliminated. In the first example, the following arbitrary beam information is used for identification:

Length: 0.09090 m	Density: 1464.5 kg/m^3
Thickness: 0.00303 m	"True" Young's modulus: 2.724 E + 10 Pa
Width: 0.0151 m	"True" Shear modulus: 1.978 E + 09 Pa

The initial values for Young's and shear modulus are obtained with formula (8) as described in Section 2.2. The frequencies calculated in MATLAB from the above-mentioned beam information are used as "virtual experimental frequencies":

f_1 1606.6 Hz f_5 18 047 Hz
f_2 4307.5 Hz f_6 23 748 Hz
f_3 8116.1 Hz f_7 29 726 Hz
f_4 12 773 Hz

From the above "virtual experimental frequencies", the identified results are listed in Table 3.

With different initial values, the identified results appeared to be the same (Table 4):

4.1.1. Discussion

This simple numerical example shows that the inverse method is capable to reproduce exactly the virtual experiments. With different initial values, as long as the same Timoshenko beam model is used, the same correct identification results can be derived.

4.2. Numerical example 2

In this example, six beams with almost the same properties except the slight changes of the transverse shear modulus are used. The properties of those beams are listed in Table 5.

The "virtual experimental frequencies" are calculated from the Timoshenko beam model by using the properties in Table 5. All results are listed in Table 6. In all the six cases, the identified values are identical to the theoretical value.

4.2.1. Discussion

From Table 6, it can be seen that even small changes of the shear modulus can be identified by the Simplex algorithm. The condition of "virtual experimental frequencies" with the correct numerical model of course remains necessary for this conclusion.

Table 3
Identified results from the frequencies of Timoshenko model

	Initial value (Pa)	Identified value (Pa)	True value (Pa)	Relative error (%)
E	2.924e10	2.724e10	2.724e10	0
G	1.518e9	1.978e9	1.978e9	0

Table 4
Identified results from the frequencies of Timoshenko model

	Initial value (Pa)	Identified value (Pa)	True value (Pa)	Relative error (%)
E	3.01e10	2.724e10	2.724e10	0
G	2.518e9	1.978e9	1.978e9	0

Table 5
Six beams with slightly different shear modulus

Beam number	Shear modulus (Pa)	Other properties	
0	1.918 e9	Length:	0.09090 m
1	1.918e9*(1+1%)	Thickness:	0.00303 m
2	1.918e9*(1+2%)	Width:	0.01515 m
3	1.918e9*(1+3%)	Density:	1464.5 kg/m^3
4	1.918e9*(1+4%)	Young's modulus:	2.724e10 pa
5	1.918e9*(1+5%)		
6	1.918e9*(1+6%)		

Table 6
Results from the six beams

	Beam 1	Beam 2	Beam 3	Beam 4	Beam 5	Beam 6
Virtual first 7 experimental frequencies (Hz)	1.6063e3	1.6064e3	1.6066e3	1.6067e3	1.6068e3	1.6070e3
	4.3077e3	4.3091e3	4.3105e3	4.3118e3	4.3132e3	4.3145e3
	8.1194e3	8.1246e3	8.1297e3	8.1347e3	8.1397e3	8.1445e3
	1.2783e4	1.2796e4	1.2808e4	1.2821e4	1.2833e4	1.2845e4
	1.8069e4	1.8094e4	1.8119e4	1.8143e4	1.8167e4	1.8190e4
	2.3785e4	2.3827e4	2.3868e4	2.3908e4	2.3948e4	2.3988e4
	2.9785e4	2.9847e4	2.9908e4	2.9969e4	3.0028e4	3.0087e4
Shear modulus changes[a] (%)	1	2	3	4	5	6
Theoretical E and G (Pa)	2.7224e10	2.7224e10	2.7224e10	2.7224e10	2.7224e 10	2.7224e10
	1.9372e9	1.9564e9	1.9755e9	1.9947e9	2.0139e9	2.0330e9
Identified E and G (Pa)	2.7225e10	2.7224e10	2.7225e10	2.7224e10	2.7224e10	2.7225e10
	1.9371e9	1.9565e9	1.9754e9	1.9948e9	2.0139e9	2.0331e9

[a]Compared with beam 0 in Table 5.

5. Experimental verification

In this section, experimentally measured frequencies of a glass beam are used to identify Young's modulus and transverse shear modulus. The error estimation is also performed so as to find the main source of errors.

5.1. Experimental test on a glass beam specimen

In this section, a real glass beam specimen is used for the experimental validation of the procedure. An error discussion is followed. Table 7 shows the geometrical and mass properties of the used beam specimen.

A glass test beam coated with reflective paint is suspended on two thin threads. This configuration simulates free–free boundary conditions. A loudspeaker and a signal generator are

used for non-contact excitation with a multisine signal. A Polytec Scanning laser Vibrometer (PSV) is used to pick up the vibration amplitudes (see Fig. 6). An experimental modal analysis is next performed using the PSV 7.1 modal analysis package to obtain mode shapes and resonance frequencies. The first seven flexural frequencies and the first four torsional frequencies are measured. The first seven flexural frequencies are used to identify the Young's modulus and the shear modulus of the glass beam test specimen with the inverse method. The consumed run time for the identification in MATLAB on a Intel Pentium III 863 MHz PC was 95.297.

The results are shown in Table 8. The measured flexural frequencies and the calculated flexural frequencies (by using the identified Young's modulus and shear modulus) are listed in Table 9.

It can be seen that in Table 9, the measured and the calculated flexural frequencies match each other very well. Their relative errors are below 0.08%. The measured torsional frequencies, the calculated torsional frequencies by using the identified material parameters in ANSYS and their relative errors are listed in Table 10. In ANSYS, the glass beam is meshed as 5*10*50 by using 20 nodes 3D elements (element type number 95). There are totally 12 531 nodes.

The first torsional frequency could not be identified with the PSV 7.1 software. Probably the excitation signal was not put in an optimal position for sufficient excitation of this mode shape. Table 10 shows that, although the material parameters are identified only from the first seven

Table 7
Geometrical and mass properties of the glass beam

Parameters	Values
Length (m)	0.30083
Width (m)	0.02993
Thickness (m)	0.00973
Mass (kg)	0.22093

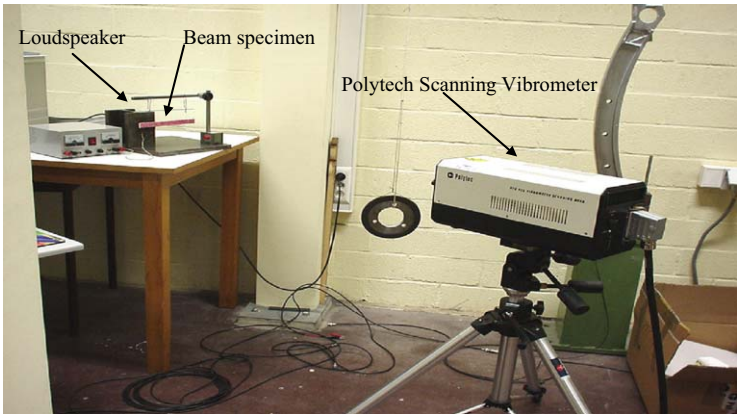

Fig. 6. Experimental setup.

Table 8
Identified parameters

Identified parameters	Values (Pa)
Young's modulus E	7.61143E + 10
Transverse shear modulus G	3.50319E + 10

Table 9
The first seven flexural frequencies

Mode order	Measured frequencies (Hz)	Calculated frequencies using identified parameters (Hz)	Relative error (%)
1	605.0	604.6330	0.0607
2	1655.0	1656.1633	−0.0703
3	3215.0	3217.4019	−0.0747
4	5260.0	5256.4159	0.0681
5	7745.0	7741.9060	0.0399
6	10 640.0	10 638.6702	0.0125
7	13 905.0	13 909.9864	−0.0359

Table 10
The first four torsional frequencies

Mode order	Measured torsional frequencies (Hz)	Calculated torsional frequencies using identified parameters (Hz) in ANSYS	Relative error (%)
1	—	3.39598E + 03	—
2	6.4675E + 03	6.81149E + 03	−5.3188%
3	9.7400E + 03	1.02652E + 04	−5.3924%
4	1.3095E + 04	1.37743E + 04	−5.1877%

flexural frequencies, the measured and calculated torsional frequencies match also in an acceptable way. Their relative errors are smaller than 5.5%. This shows that the identified material parameters are reliable. The layer of reflective paint and the suspension threads probably contributed to discrepancies between the measured and computed values.

5.2. Error estimation for the moduli obtained with the glass beam test

The proposed method in Section 3.1 is applied to the tested glass beam in Section 5.1. The values and the uncertainties on the input parameters are listed in Table 11.

In Table 11, the uncertainty interval of the length, width and thickness is determined by the used electronic vernier calliper with an accuracy of 0.01 mm; the uncertainty interval of mass is determined by the used electronic balance with an accuracy of 0.01 g; the uncertainty interval of frequencies is determined by the following facts: (1) the test specimen has good homogeneous material properties; (2) machined with proper care; (3) the non-contact excitation with the loudspeaker and the non-contact measurement with the laser vibrometer on the freely suspended glass beam; (4) last, but not least, the long-time repeated testing with careful observation.

It can be remarked that the selected error intervals in Table 11 are taken very small. This is only allowed if the test specimen has good homogeneous material properties and if it is machined with proper care. Also, the non-contact excitation with the loudspeaker and the non-contact measurement with the laser vibrometer on the freely suspended glass beam justify the assumed small error intervals on the measured frequencies. Based on these intervals and the computed sensitivities, it is possible to estimate uncertainty intervals on the obtained material properties by formulas (11) and (13).

The computed uncertainty intervals for the identified material properties are listed in Table 12.

According to Eq. (13) in Section 3.1, the relative contributions of the computed uncertainty of the input parameters are listed in Table 13.

Table 11
The values and the uncertainty on the input parameters

	Value	Uncertainty interval	Absolute error
Freq-1 (Hz)	605.0	604.9–605.1	±0.1
Freq-2 (Hz)	1655.0	1654.9–1655.1	±0.1
Freq-3 (Hz)	3215.0	3214.9–3215.1	±0.1
Freq-4 (Hz)	5260.0	5259.5–5260.5	±0.5
Freq-5 (Hz)	7745.0	7744.5–7745.5	±0.5
Freq-6 (Hz)	10 640.0	10 639–10 641	±1
Freq-7 (Hz)	13 905.0	13 904–13 906	±1
Length (mm)	300.83	300.82–300.84	±0.01
Width (mm)	29.93	29.92–29.94	±0.01
Thickness (mm)	9.73	9.72–9.74	±0.01
Mass (g)	220.93	220.92–220.94	±0.01

Table 12
The uncertainty interval for the identified material property

	Value	Uncertainty interval	Abs. error	Rel. error (%)
E (GPa)	76.0872	75.8856–76.2888	±0.201600	0.2650
G (Gpa)	34.5621	34.364217–34.75998	±0.197883	0.5725

Table 13
The relative contributions of the uncertainty of the input parameters

	Freq-1 (%)	Freq-2 (%)	Freq-3 (%)	Freq-4 (%)	Freq-5 (%)	Freq-6 (%)	Freq-7 (%)	Length (%)	Thickness (%)	Width (%)	Mass (%)
E	0.13981	0.3478	0.5738	3.5823	3.3395	3.2070	5.2247	5.0210	76.8397	0.0036	1.7207
G	0.6931	1.7079	2.7650	16.5899	13.9237	5.8602	43.5292	0.4872	13.7333	0.0246	0.6859

From the above results, it can be seen that (1) the relative error on G is more than two times the relative error on E for the same assumed levels of uncertainty; (2) the accuracy of the thickness is crucial for the uncertainty levels on Young's modulus; (3) the accuracy of the measured four highest frequencies is very important for the accuracy on the transverse shear modulus. This stresses the fact that it is necessary to measure the higher-order flexural frequencies with high accuracy; (4) the accuracy of the thickness measurement has also considerable influence on the identified shear modulus.

6. Conclusion

In this paper, it was shown that relatively short beams (low length-to-thickness ratio) with a low value of the transverse shear modulus G (as compared with Young's modulus), have a considerable influence of the transverse shear modulus on their flexural resonance values. This is especially true for high mode shape numbers.

The paper also showed that it is possible to identify Young's modulus and transverse shear modulus with an inverse method, based on measured flexural resonance frequencies. The proposed procedure can identify the transverse shear modulus and Young's modulus from the flexural vibration frequencies of beams with rectangular cross-section with an acceptable uncertainty interval. The proposed procedure was illustrated with numerically simulated "virtual measurements" and next applied to a real experiment. Formulas to assess the uncertainty estimation were derived and graphically illustrated.

It appeared that the accuracy of the measured specimen thickness has a large influence on the identical material to Young's modulus. It also appeared that the accuracy of the measured high-order frequencies is crucial to the uncertainty interval on the identified transverse shear modulus.

Acknowledgements

This work was performed in the framework of the inter university research project called "GRAMATIC" between the Katholic Univerity of Leuven and the Free University of Brussels, both situated in Flanders, Belgium. The project is financially supported by the Flemish Institute IWT for the promotion of Scientific and Technological Research in Industry.

References

[1] J.A. Wolf, T.G. Carne, Identification of the elastic constants for composites using modal analysis, *Proceedings of the Society for Experimental Stress Analysis*, San Francisco, CA, USA, 1979.

[2] W.P. De Wilde, H. Sol, Determination of the material constants of an anisotropic lamina by free vibration analysis, *Proceedings of the Second International Modal Analysis Conference*, Orlando, FL, USA, 1984

[3] W.P. De Wilde, H. Sol, Coupling of Lagrange interpolation, modal analysis and sensitivity analysis in the determination of anisotropic plate rigidities, *Proceedings of the Fourth International Modal Analysis Conference*, Orlando, FL, USA, 1986.

[4] H. Sol, Identification of Anisotropic Plate Rigidities Using Free Vibration Data, Ph.D Thesis, Free University of Brussels, Belgium 1986.

[5] L.R. Deobald, Determination of Elastic Constants of Orthotropic Plates by a Modal Analysis/Rayleigh–Ritz Technique, Master Thesis, University of Idaho, 1985.

[6] L.R. Deobald, R.F. Gibson, Determination of elastic constants of orthotropic plates by a modal analysis/ Rayleigh–Ritz technique, *Proceedings of the Fourth International Modal Analysis Conference*, Los Angeles, FL, USA, 1986.

[7] P.S. Frederiksen, Identification of Material Parameters in Anisotropic Plates, A Combined Numerical/ Experimental Method, PhD Thesis, Department of Solid Mechanics, Technical University of Denmark, 1992.

[8] T.G. Garne, A.R. Martinez, Identification of material constants for a composite structure, *Proceedings of the Ninth International Modal Analysis Conference*, Italy, 1991, pp. 660–670.

[9] F. Moussu, M. Nivoit, Determination of elastic constants of orthotropic plates by a modal analysis/method of superposition, *Journal of Sound and Vibration* 165 (1993) 149–163.

[10] T.C. Lai, K.H. Ip, Parameter estimation of orthotropic plates by Bayesian sensitivity analysis, *Composite Structures* 34 (1999) 29–42.

[11] H. Hua, Identification of Plate Rigidities of Anisotropic Rectangular Plates, Sandwich Panels and Circular Orthotropic Disks Using Vibration Data, PhD thesis, Free University of Brussels, Belgium, 1993.

[12] P.S. Frederiksen, Experimental procedure and results for the identification of elastic constants of thick orthotropic plates, Internal Report No. 506, Danish Centre for Applied Mathematics and Mechanics, 1995.

[13] P.S. Frederiksen, Single-layer plate theories applied to the flexural vibration of completely free thick laminates, *Journal of Sound and Vibration* 186 (1995) 743–759.

[14] V. Marchand, J. Authesserre, Determination of the elastic constants of material, in the form of plates, by a free vibration method, *Journal of Sound and Vibration* 194 (1996) 497–512.

[15] M. Grédiac, P.A. Paris, Direct identification of elastic constants of anisotropic plates by modal analysis: theoretical and numerical aspects, *Journal of Sound and Vibration* 195 (1996) 401–415.

[16] W.T. Wang, T.Y. Kam, Determination of elastic constants of composite laminates using measured natural frequencies, *Advances in Composite Materials and Structures*, Vol. VII, 2000, pp. 95–104.

[17] S.F. Hwang, C.S. Chang, Determination of elastic constants of materials by vibration testing, *Composite Structures* 49 (2000) 183–190.

[18] R. Rikards, A. Chate, G. Gailis, Identification of elastic properties of laminates based on experiment design, *International Journal of Solid and Structures* 38 (2001) 5097–5115.

[19] G.R. Liu, K.Y. Lam, X. Han, Determination of elastic constants of anisotropic laminated plates using elastic waves and a progressive neutral network, *Journal of Sound and Vibration* 252 (2002) 239–259.

[20] Standard test method for dynamic Young's modulus, shear modulus, and Poisson's ratio for advanced ceramics by impulse excitation of vibration. Designation: C 1259–1298.

[21] P.O. Larsson, Determination of Young's and shear moduli from flexural vibration of beams, *Journal of Sound and Vibration* 146 (1991) 111–123.

[22] A. Wanner, K. Kromp, Young' and shear moduli of laminated carbon/carbon composites by a resonant beam method, in: A.M. Brandt, I.H. Marshall (Eds.), *Brittle Matrix Composites 2*, Elsevier, London, 1988, pp. 280–289.

[23] W. Lins, G. Kaindl, et al., A novel resonant beam technique to determine the elastic moduli in dependence on orientation and temperature up to 2000°, *Review of Scientific Instruments* 70 (1999) 3052–3058.

[24] J.C. Lagarias, J.A. Reeds, M.H. Wright, P.E. Wright, Convergence properties of the Nelder Mead simplex method in low dimensions, *SIAM Journal on Optimization* 9 (1998) 112–147.
[25] D. Moens, A Non-probabilistic Finite Element Approach for Structural Dynamic Analysis With Uncertainty Parameters. PhD Thesis, Katholieke Universiteit Leuven, Belgium 2002.
[26] S.H. Chen, H.D. Lian, X.W. Yang, Interval eigenvalue analysis for structures with interval parameters, *Finite Elements in Analysis and Design* 39 (2003) 419–431.
[27] M. Hanss, A. Klimke, *On the relability of the influence measure in the transformation method of fuzzy arithmetic. Fuzzy Sets and Systems* 143 (2004) 371–390.
[28] T. Lauwagie, G. Roebben, H. Sol, W. Heylen, O. Van der Biest, The uncertainty budget of Mixed-Numerical-Experimental-Techniques for the identification of elastic material properties from resonance vibrations, *Proceedings of ISMA 2004, International Conference on Noise and Vibration Engineering,* Leuven, Belgium, 20–22 September 2004.